Desalination and Water Treatment
www.deswater.com

doi:10.5004/dwt.2017.20717

76 (2017) 121–133
May

Fouling behavior investigation of a thermally modified RO membrane

Afarin Djavanrouh[a], Toraj Mohammadi[a,*], Omid Bakhtiari[b]

[a]*Research and Technology Centre for Membrane Processes, Faculty of Chemical Engineering, Iran University of Science and Technology (IUST), Narmak, Tehran, Iran, Tel. +98 21 77 240 051, Fax +98 21 77 240 051, email: afarin.djavanrouh@yahoo.com (A. Djavanrouh), Tel. +98 21 77 240 051, Fax +98 21 77 240 051, email: torajmohammadi@iust.ac.ir (T. Mohammadi)*
[b]*Membrane Research Centre, Faculty of Petroleum and Chemical Engineering, Razi University, Kermanshah, Iran, Tel. +98 83 34 283 262, Fax +98 83 34 283 262, email: obakhtiari@razi.ac.ir (O. Bakhtiari)*

Received 13 October 2016; Accepted 16 March 2017

ABSTRACT

The main aim of present study is to investigate performance and fouling/cleaning behavior of reverse osmosis membranes and study heat treatment effect(s)as a membrane surface modification method on the membranes separation performance. For this purpose, performance of the reverse osmosis membranes as permeation flux, and Na and Mg rejections was investigated using response surface methodology (RSM) as functions of four main variables including trans-membrane pressure (TMP, bar), operating temperature (T, °C), cross flow (CF, $L{\cdot}h^{-1}$) and total dissolved solids (TDS, $mg{\cdot}L^{-1}$). Also, another RSM design was used to study the membrane fouling/cleaning behavior, i.e. the response of permeation flux recovery, vs. the variables of cross flow (CF, $L{\cdot}h^{-1}$), pH and cleaning time (t, min). Effects of the membrane surface modification via the heat treatment on its fouling resistance and cleaning performance were also investigated. The membranes were modified via washing with deionized water followed by immersing in deionized water at 70°C for 3 h and then maintaining in deionized water at 4°C and dark ambient until evaluation. The membranes' fouling resistance during 20 h operation and their fouling/cleaning behavior using synthetic foulant down to 80% of their initial permeation fluxes were determined at the experimentally obtained optimum conditions of fouling/cleaning cycles for both the modified and non-modified membranes. The optimum performance of the membrane with permeation flux of 59.1 $kg{\cdot}m^{-2}{\cdot}h^{-1}$ and Na and Mg rejections of 99.3 and 95.0% was identified at TMP, T, CF and TDS of 17 bar, 35°C, 1200 $L{\cdot}h^{-1}$ and 10000 $mg{\cdot}L^{-1}$, respectively. Also, the optimum permeation flux recovery was determined as 94% at CF of 250 $L{\cdot}h^{-1}$,pH of 10 and cleaning time of 45 min. Permeation flux decline of the non-modified membrane was about 20%, while that of the modified membrane was found very lower as 3%. Also, the solutes rejection values were slightly increased from 99.3 to 99.4% and from 95.0 to 95.2% for Na and Mg, respectively for the modified membrane. In addition, it took about 3 h for the non-modified membrane and approximately 12 h for the modified membrane to be fouled as BSA added as foulant by 200 $mg{\cdot}L^{-1}$ BSA to the sodium chloride and magnesium sulfate aqueous solution of 10000 $mg{\cdot}L^{-1}$. Cleaning of the fouled membranes was performed and permeation flux recovery for the non-modified membrane was measured as 94.0% and for the modified membranes as 94.1%.

Keywords: Reverse osmosis membrane; Fouling/cleaning behavior; Heat treatment; Experimental design

*Corresponding author.

1. Introduction

Significant part of the world's water is seawater, brackish water and groundwater and available fresh water is less than 0.014% of total world's water amount [1,2]. However, fresh water has been significantly reduced due to its high consumption resulted from population growth, rapid urban sprawl, agriculture development, industrialization, and tourism industry [1,3–6]. Accordingly, new desalination technologies for supplying drinking water form brackish water gained more attention recently due to its low operating cost and energy requirement [1,4]. Brackish water is mainly includes sodium chloride (NaCl) and magnesium sulfate ($MgSO_4$) salts.

Reverse osmosis (RO) is one of the leading technologies in fresh water production [7–12]. In this process, high pressure salty water flows over a semi-permeable membrane through where pure water passes and salt and other impurities are rejected [7,13–15]. The membrane performance is influence directly by permeation flux and salt rejection [7,14,15]. There are different variables affect the membrane performance including trans-membrane pressure (TMP), temperature (T), cross flow velocity(CF) and the feed's total dissolved solids (TDS). However, in this process rejected impurities and salts were accumulated over the membrane surface known as concentration polarization phenomenon [4,7,12,14,15]. This ultimately leads to the membrane fouling that results in more energy consumption in order to keep the membrane's water flux constant [4,7,16] and also the membrane life's shortening [7,14,15]. Consequently, the membrane cleaning investigations for restoring the membrane performance and the membrane surface modifications for delaying the membrane fouling are essential requirements [4,7]. Some variables which influence the membrane fouling/cleaning are such as cross flow (CF), pH and time (t).

Most commercially RO membranes have thin polyamide active skin layers on top of porous supporting layers. Permeation flux, salts rejection and fouling capacity of RO membranes are determined by their active skin layers characteristics [4,17]. Also, spacers are placed between the membranes in order to keep them separated from each other and increase their performance by enhancing the momentum mixing and reducing the concentration polarization [7,18]. On the other hand, there are some physical and chemical modification approaches on the active skin layers of commercial RO membranes. Physical modifications are based on adsorption, coating and heat treatment, while chemical modifications include hydrophilization, radical grafting, chemical coupling and plasma polymerization [17]. In fact, higher hydrophilicity of the active skin layer leads to lower fouling tendency due to the reduced membrane surface's salts adsorption [4,19,20]. Heat treatment also improves the membrane performance by changing the active skin layer's free-volume and the membrane surface roughness [3,4,21].

In this study, performance of some RO membranes as permeation flux, and Na and Mg cations' rejections and their cleaning as permeation flux recovery were studied. Also, the membrane surface modification via heat treatment was investigated and its fouling resistance in comparison with the non-modified membrane was investigated. Effects of different variables on the RO membranes' performance and their fouling/cleaning tendencies were also investigated. Finally, the target variables were predicted using response surface methodology (RSM) by central composition design (CCD) and the predictions were compared with those of experimentally measured values.

2. Material

2.1. Membrane

In the all experiments, polyamide membrane pieces of CSM brackish water (RE2521-BE model) from Korea were used as the testing RO membrane. Some of its characteristics, as reported by the manufacturer, are presented in Table 1.

2.2. Process feed

Some aqueous solutions of NaCl and $MgSO_4$ salt mixtures with the ratio of 1 to 4 were used as the feed solutions. The salts were provided by Labchimi, India. Homemade deionized water was prepared using a Milli-Q purification system (Millipore Corp).

2.3. Foulant and cleaning agents

BSA with 200 $mg \cdot L^{-1}$ purchased from Merck Co. was added to the sodium chloride and magnesium sulfate solution with concentration determined by experimental design and this mixture was used as a dirty fouling feed solution. Also, sodium hydroxide (NaOH) and citric acid (CA) were used as chemical cleaning agents. They were purchased from Ghatranchimi, Iran.

3. Experimental

3.1. Theory

3.1.1. Permeation flux and solutes rejection mechanisms

Two main important performance characteristics of RO membrane separation process are permeation flux and solute rejection. Permeation flux indicates the amount of permeate and the product rate and solute rejection is also utilized in order to present RO efficiency for desalination. After steady state was attained (5 h), permeation flux was measured gravimetrically with an electronic balance via weighting the permeation. It was calculated using Eq. (1).

$$PF = \frac{V}{A \times t} \tag{1}$$

Table 1
Characteristics of the polyamide RO membrane

Membrane		Recommended operating limits		
Name	Material	pH range	Pressure range (bar)	Temperature range (°C)
CSM brackish water	Polyamide (PA)	2–11	< 41.4	< 45

where V is volume of the collected permeated stream, A is the effective membrane surface area and t is the permeation time. Rejection of different solutes were calculated by comparing their concentrations in the feed and the permeate sides, as the follows:

$$\text{Rejection } (\%) = \frac{C_f - C_p}{C_f} \times 100 \quad (2)$$

where C_f and C_p are the salute concentrations in the feed and permeate sides.

3.1.2. Cleaning mechanism

A fouling cake/gel layer is formed on the membrane surface and cleaning reagents diffuse through it. A chemical reaction takes place between the cleaning reagents and the deposited materials in the fouling layer which leads to weaken them. Then the products diffuse back from the membrane surface to the bulk of cleaning feed solution. The reaction may be hydrolysis, dissolution or dispersion[22]. These finally results the deposited materials removal from the membrane surface. At this time, permeation flux recovery can be calculated using the following equation:

$$\text{Permeation flux recovery } (\%) = 1 - \frac{PF_{BF} - PF_{AC}}{PF_{BF}} \times 100 \quad (3)$$

where PF_{BF} is permeation flux before fouling and PF_{AC} is permeation flux after cleaning.

3.1.3. Heat treatment

Fouling resistance of commercially available polyamide low pressure RO membranes can also be improved by heat treatment. In fact, interactions between physicochemical characteristics of RO membranes surface and foulants decrease after heat treatment. To thermally treat the membrane samples, they were firstly washed with deionized water to eliminate any preservative chemicals from the membrane surface. Then, they were immersed in deionized water at 70°C for 3 h. Consequently, the modified membrane samples were maintained in deionized water at 4°C in dark ambient until their experimental evaluation [4]. The modified membrane samples fouling resistance before and after heat treatment and fouling/cleaning behavior were studied at the optimum condition resulted from related experimental design. Fouling resistance was investigated during 20 h and cleaning was performed when permeation flux reduces down to 80% of its initial value.

3.2. Analysis of samples

The total dissolved solids (TDS) contents of feed and the permeate samples were measured using the Mytrrvhm 761 Compact ion chromatography (IC) devices with 300 anion column Star-Ion-pack.

3.3. The lab scale plant

As shown in Fig. 1, an experimental setup almost close to an industrial scale was used to perform the experiments.

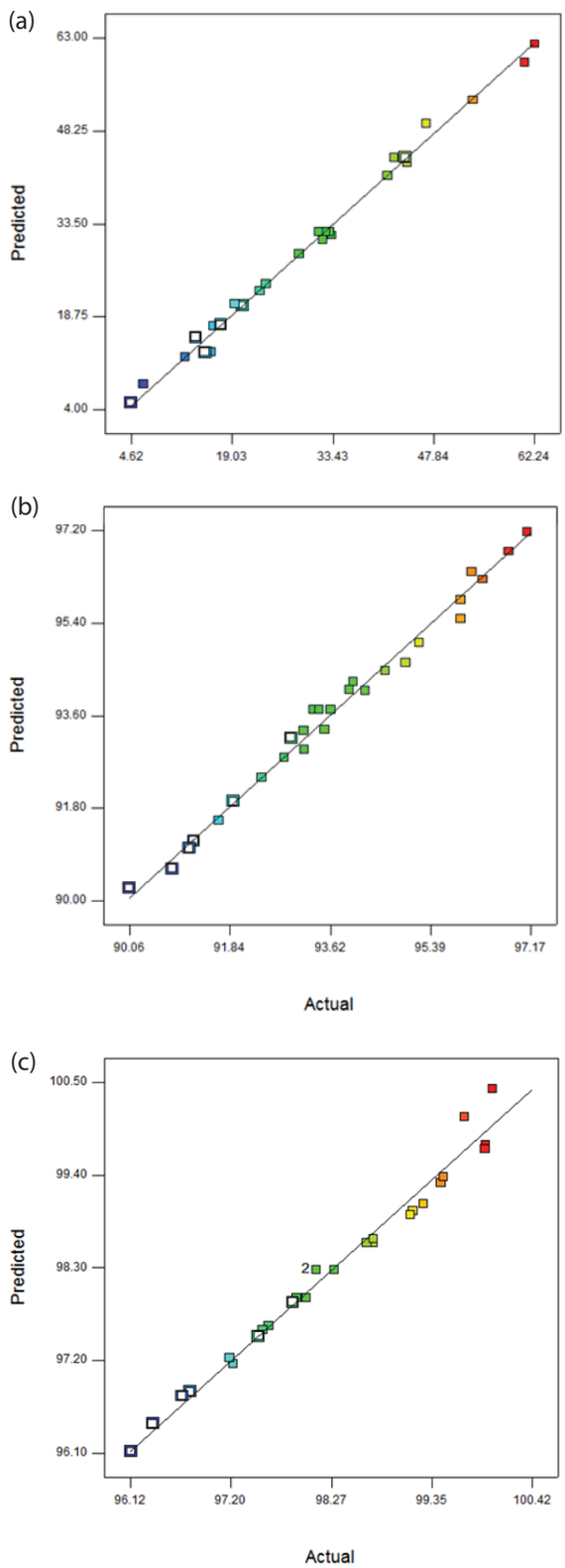

Fig. 1. Scatter diagram of predicted response vs. actual response for performance of the membrane. a) Permeation flux, b) Na rejection and c) Mg rejection.

It has ability to tune and control all the important operating parameters. The system was operated in a cross flow mode. Consequently the feed stream did tangentially flow on the membrane surface and only a small part of the feed was processed through the membrane. The membrane's effective surface area in the feed side was equal to 0.0038 m^2. The experimental setup consists of a vessel with a capacity of 10 L with a tubular heat exchanger in order to control the feed temperature and also a stirrer in order to keep the feed uniform. The feed temperature was measured by a digital thermometer with an accuracy of ± 0.1°C.

3.4. Membrane characterization

Surface roughness, topography and morphology of the prepared membranes were evaluated by atomic force microscopy (AFM) using Full Plus, Ara Pazhohesh Co.

3.5. Experimental design

RSM as a statistical and mathematical method was utilized to investigate the variables effects on the response. It determines significance of the variables on the response and obtains a correlation between the variables and the response(s) based on experimental data with minimum number of experiments. Also, it determines the optimum values of the investigated variables to obtain the best desired response(s) [23]. Thus, a model was built to describe the response as defined by Eq. (2). Design-Expert 7.0.0 software (2015) was used to calculate the equation as the follows:

$$Y = \beta_0 + \sum_{j=1}^{k} \beta_j x_j + \sum_{j=1}^{k} \beta_{jj} x_j^2 + \sum_{i} \sum_{<j=2}^{k} \beta_{ij} x_i x_j + e_i \quad (4)$$

where, Y is the predicted response, β_0 is a constant coefficient, β_j is a linear coefficient, β_{jj}s are quadratic coefficients, β_{ij}s are the interaction coefficients, k is the number of factors, x_i and x_j represent the independent factors, and e_i is prediction error. Analysis of Variance (ANOVA) was also performed in order to model the results of statistical analysis. Model fitting quality with experimental data was studied by F-value, P-value, R^2, and lack of fit [23,24]. Performance of the membrane was studied using four variables including trans-membrane pressure (bar), temperature °C, cross flow (L·h^{-1}) and total dissolved solids (mg·L^{-1}) each with five levels and responses were as permeation flux, and Na and Mg cations rejections. Also, cleaning of the membrane was investigated using cross flow (L·h^{-1}), pH and time (min) at five levels and response was permeation flux recovery, as presented in Table 2. Furthermore, Tables 3 and 4 illustrate the CCD experimental design provided by Design Expert software (version 7.0. 0) for membrane performance and cleaning, respectively.

Table 3
CCD for performance of the membrane

Run	TMP (bar)	T (°C)	CF (L·h^{-1})	TDS (mg·L^{-1})	Permeation flux (kg·m^{-2}·h^{-1})	Rejection (%)	
						Na	Mg
1	17	25	1200	5000	42.1	96.7	99.6
2	13	30	800	7500	31.4	93.6	98.3
3	17	35	1200	10000	46.7	94.5	99.1
4	9	35	1200	5000	23.0	91.6	97.2
5	13	30	800	2500	31.9	94.0	98.7
6	17	35	400	10000	44.0	94.2	98.7
7	13	30	800	7500	32.8	93.3	98.1
8	17	25	400	5000	41.2	96.1	99.9
9	13	30	800	12500	17.4	92.9	97.8
10	13	30	1600	7500	31.9	93.9	98.6
11	21	30	800	7500	62.2	97.1	99.9
12	5	30	800	7500	4.6	90.1	96.1
13	9	35	400	5000	13.8	91.2	96.7
14	9	25	400	5000	16.0	93.1	97.6
15	13	30	800	7500	32.3	93.4	98.1
16	13	40	800	7500	43.7	91.8	97.4
17	17	35	1200	5000	60.8	95.2	99.4
18	9	25	1200	10000	12.3	92.8	97.5
19	13	30	0	7500	19.4	93.1	97.9
20	9	25	400	10000	6.4	92.4	97.1
21	17	25	1200	10000	33.3	96.3	99.9
22	9	25	1200	5000	16.4	93.5	98.0
23	9	35	1200	10000	20.5	91.1	96.6
24	13	20	800	7500	23.9	95.9	99.2
25	9	35	400	10000	15.1	90.8	96.3
26	17	35	400	5000	53.4	94.9	99.1
27	17	25	400	10000	28.6	95.9	99.4

Table 2
Experimental variables and their levels

	Variables (unit)	Symbol	Levels				
			–2	–1	0	1	2
Performance of the membrane	Trans-membrane pressure (bar)	TMP	5	9	13	17	21
	Temperature (°C)	T	20	25	30	35	40
	Cross flow (L·h^{-1})	CF	0	400	800	1200	1600
	Total dissolved solids (mg·L^{-1})	TDS	2500	5000	7500	10000	12500
Cleaning of the membrane	Cross flow (L·h^{-1})	CF	100	150	200	250	300
	pH	pH	3	5	7	9	11
	Time (min)	t	5	15	25	35	45

Table 4
CCD for cleaning of the membrane

Run	CF ($L \cdot h^{-1}$)	pH	*t* (min)	Permeation flux recovery (%)
1	250	5	35	63.1
2	250	5	15	57.8
3	150	9	35	70.8
4	250	9	15	55.9
5	150	9	15	42.8
6	150	5	35	55.9
7	200	7	25	52.3
8	200	7	25	50.7
9	250	9	35	73.9
10	300	7	25	60.2
11	200	3	25	77.0
12	200	7	45	65.2
13	150	5	15	40.8
14	100	7	25	41.0
15	200	7	5	27.0
16	200	11	25	89.4
17	200	7	25	50.5

4. Results and discussion

4.1. Characterization

As illustrated in Fig. 1, heat treatment results in membrane surface roughness increment from 26.2 nm (non-modified) to 39.0 nm (modified). In fact, heat treatment results in physical changes in the membrane surface which are regard to the polymeric matrix of the cross linked active skin layer contraction. This is in agreement with the observation in the other literature [3,4].

4.2. Design of experiments using CCD

The experimental results for performance and fouling/cleaning of the membrane are also presented in Tables 3 and 4, respectively. The regression equations for calculating the responses in terms of the selected symbols for the variables are presented as follows:

$$\begin{aligned}\text{Permeation flux} = {} & 5.86200 + 1.00351\ \text{Press} - 2.31539 \\ & \times \text{Temp} + 0.012782 \times \text{Flow} + 3.78558\text{E-}003 \times \text{TDS} + 0.11940 \\ & \times \text{Press} \times \text{Temp} - 2.00909\text{E-}004 \times \text{Press} \times \text{Flow} \\ & - 1.87817\text{E-}004 \times \text{Press} \times \text{TDS} + 3.95304\text{E} - 004 \\ & \times \text{Temp} \times \text{Flow} + 5.25614\text{E-}005 \times \text{Temp} \times \text{TDS} \\ & + 4.23419\text{E-}008 \times \text{Flow} \times \text{TDS} + 0.020968 \times \text{Press}^2 + 0.017658 \\ & \times \text{Temp}^2 - 9.95663\text{E-}006 \times \text{Flow}^2 - 2.95570\text{E-}007 \times \text{TDS}^2\end{aligned} \quad (5)$$

$$\begin{aligned}\text{Rejection Na} = {} & 93.82985 + 0.43230 \times \text{Press} - 0.17738 \\ & \times \text{Temp} + 4.95104\text{E-}004 \times \text{Flow} - 1.08817\text{E-}004 \times \text{TDS}\end{aligned} \quad (6)$$

$$\begin{aligned}\text{Rejection Mg} = {} & 97.366911 + 0.268655208 \times \text{Press} \\ & - 0.078359167 \times \text{Temp} + 0.000410844 \times \text{Flow} \\ & - 7.55167\text{E-}05 \times \text{TDS}\end{aligned} \quad (7)$$

$$\begin{aligned}\text{Permeation flux recovery} = {} & 70.04496 + 0.32568 \times \text{Flow} \\ & - 27.31033 \times \text{pH} + 1.39549 \times \text{Time} - 0.013870 \times \text{Flow} \times \text{pH} \\ & - 4.23900\text{E-}003 \times \text{Flow} \times \text{Time} + 0.14185 \times \text{pH} \times \text{Time} \\ & - 5.09413\text{E-}005 \times \text{Flow}^2 + 2.00201\ \text{pH}^2 - 0.012611 \times \text{Time}^2\end{aligned} \quad (8)$$

4.3. Analysis of variance study

ANOVA results related to performance of the membrane are presented in Table 5. Significant model terms for permeation flux are A, B, C, D, AB, AD, C^2 and D^2 which their P-values are lower than 0.05 and others, those have P-value greater than 0.1, are not significant. It means that these coefficients are more significant than the others. However, just A, B, C and D are significantly effective on the rejection responses. As shown in Table 5, the high model F-values and the low model P-values for the regression models show that the models are entirely significant. Also, the Lack of Fit values are not significant relative to the pure error. The adjusted R^2 (R^2_{adj}) and the predicted R^2 (R^2_{pre}) are in good agreement. Adequate precision is a measure of the range in predicted response relative to its associated error. The proper value is 4 or higher and as it can be seen, the calculated values are higher than 4, demonstrating that the models are proper for the statistical design and data analysis.

ANOVA results related to cleaning of the membrane are presented in Table 6. Significant model terms are A, B, C, D, E, F, AB, AC, BC, B^2 and C^2. The high F-value and the low P-value for the regression model show significance of the model. The Lack of Fit F-value presents it is not significant compared with the pure error. The R^2_{adj} and R^2_{pre} values are also in good agreement. Also, high adequate precision ratio illustrates that the model is appropriate in order to performing the statistical design and the data analysis.

The predicted response versus the actual response for performance and cleaning of the membrane are shown in Figs. 2 a–c and Fig. 3, respectively. In these graphs as the data points become closer to the 45° line, the agreement between model and experimental data is more appropriate. As observed, the data points are very close to the 45° line and thus the models can predict the experimental data very well.

4.4. Performance of the membrane

4.4.1. The Effect of TMP

Effect of TMP on permeation flux is shown in Figs. 4 a–c. Based on Darcy's law, increasing TMP leads to permeation flux increment due to the bigger driving force [25], however, it blocks the membrane surface due to cake/gel layer formation resulted from more compaction of sediments [26,27]. Hence, at an optimum TMP, permeation flux is high, while tendency to cake/gel layer formation is low. It can be observed that, as TMP increases up to 17 bar, permeation flux increases sharply, while further increasing TMP is not effective and economical. This can be due to the less cake/gel layer formation tendency on the membrane surface at this pressure range. Also as it illustrated in Fig. 5a, increasing TMP increases solutes rejections [28]. It is due to the higher compactness of sediments on the

Table 5
ANOVA results of the quadratic model for performance of the membrane

Source	Permeation flux (kg·m^{-2}·h^{-1})		Na rejection (%)		Mg rejection (%)		Remark
	F Value	P-value	F Value	P-value	F Value	P-value	
Model	135.9933	< 0.0001	499.4601	< 0.0001	282.1039	< 0.0001	Significant
A-press	1473.4350	< 0.0001	1535.7230	< 0.0001	950.5038	< 0.0001	
B-temp	183.9712	< 0.0001	403.9644	< 0.0001	126.3464	< 0.0001	
C-flow	47.8177	< 0.0001	20.1433	0.0002	22.2288	0.0001	
D-TDS	99.2455	< 0.0001	38.0092	< 0.0001	29.3365	< 0.0001	
AB	27.6031	0.0002					
AC	0.5001	0.4929					
AD	17.0745	0.0014					
BC	3.0255	0.1075					
BD	2.0894	0.1739					
CD	0.0086	0.9273					
A^2	0.7263	0.4107					
B^2	1.2576	0.2840					
C^2	16.3788	0.0016					
D^2	22.0240	0.0005					
Lack of fit	7.1506	0.1288	2.1029	0.3716	2.5348	0.3209	Not significant
R^2	0.9937		0.9891		0.9808		
Adj R^2	0.9864		0.9871		0.9773		
Pred R^2	0.9645		0.9840		0.9706		
Adeq precision	42.0490		74.3545		58.4962		

Table 6

ANOVA results of the quadratic model for cleaning of the membrane

Source	F value	P-value	Remark
Model	345.3288	< 0.0001	Significant
A-flow	342.3782	< 0.0001	
B-pH	116.3531	< 0.0001	
C-time	1085.2050	< 0.0001	
AB	12.6028	0.0093	
AC	29.4294	0.0010	
BC	52.7271	0.0002	
A^2	0.2572	0.6276	
B^2	1017.1160	< 0.0001	
C^2	25.2244	0.0015	
Lack of fit	1.3453	0.4783	Not significant
R^2	0.9977		
Adj R^2	0.9948		
Pred R^2	0.9847		
Adeq precision	72.2536		

membrane surface which restricts solutes transfer, while water is transfers more rapidly at higher TMP [29]. In fact, tendency to cake/gel layer formation leads to less solutes transfer. Hence, TMP of 17 bar was selected as the optimum value for providing high permeation flux and also high solutes rejections.

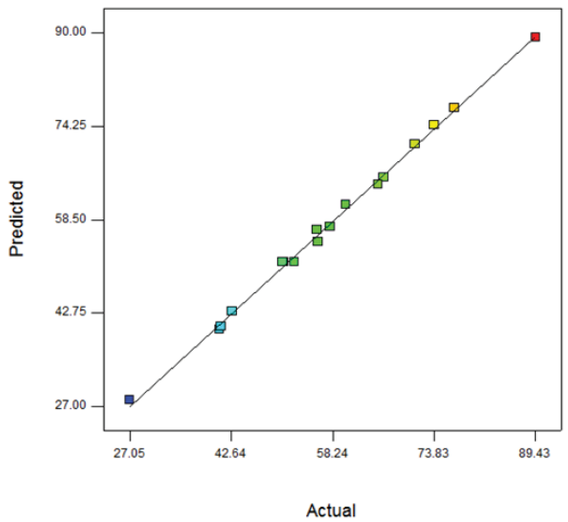

Fig. 2. Scatter diagram of predicted response vs. actual response for cleaning of the membrane.

4.4.2. Effect of the operating temperature

Effects of the operating temperature on performance of the membrane are presented in Fig. 4b. The operating temperature has two different effects on the membrane performance. Increasing temperature based on Darcy's law leads to osmotic pressure increment and reduction in the permeation flux [26]. However, this decreases viscosity and

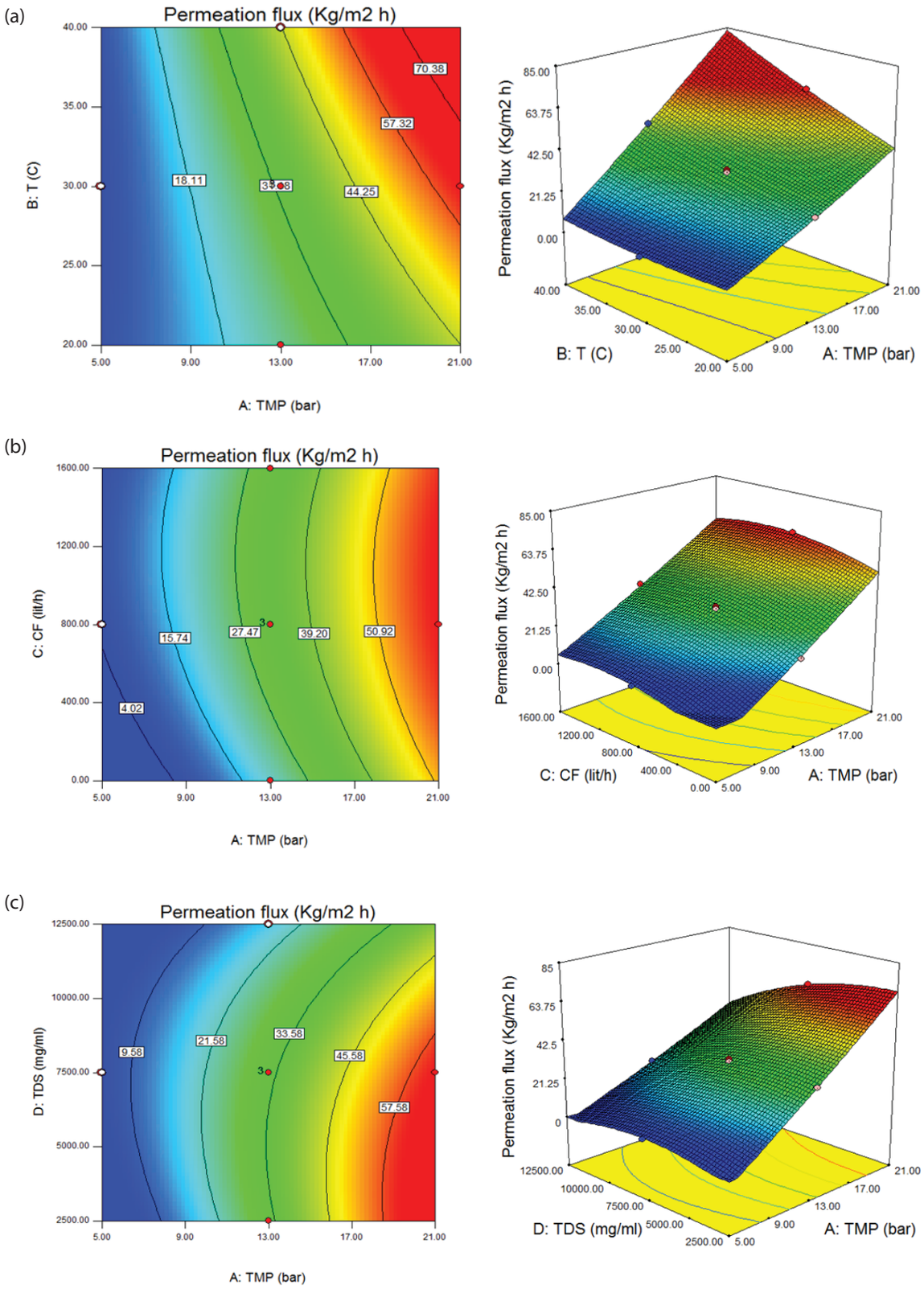

Fig. 3. Effects of TMP, T, CF and TDS on performance of the membrane (permeation flux) a) CF = 12000L·h^{-1} and TDS = 7500 mg·L^{-1}, b) T = 35°C and TDS = 7500 mg·L^{-1} and c) T = 35°C and CF = 12000 L·h^{-1}.

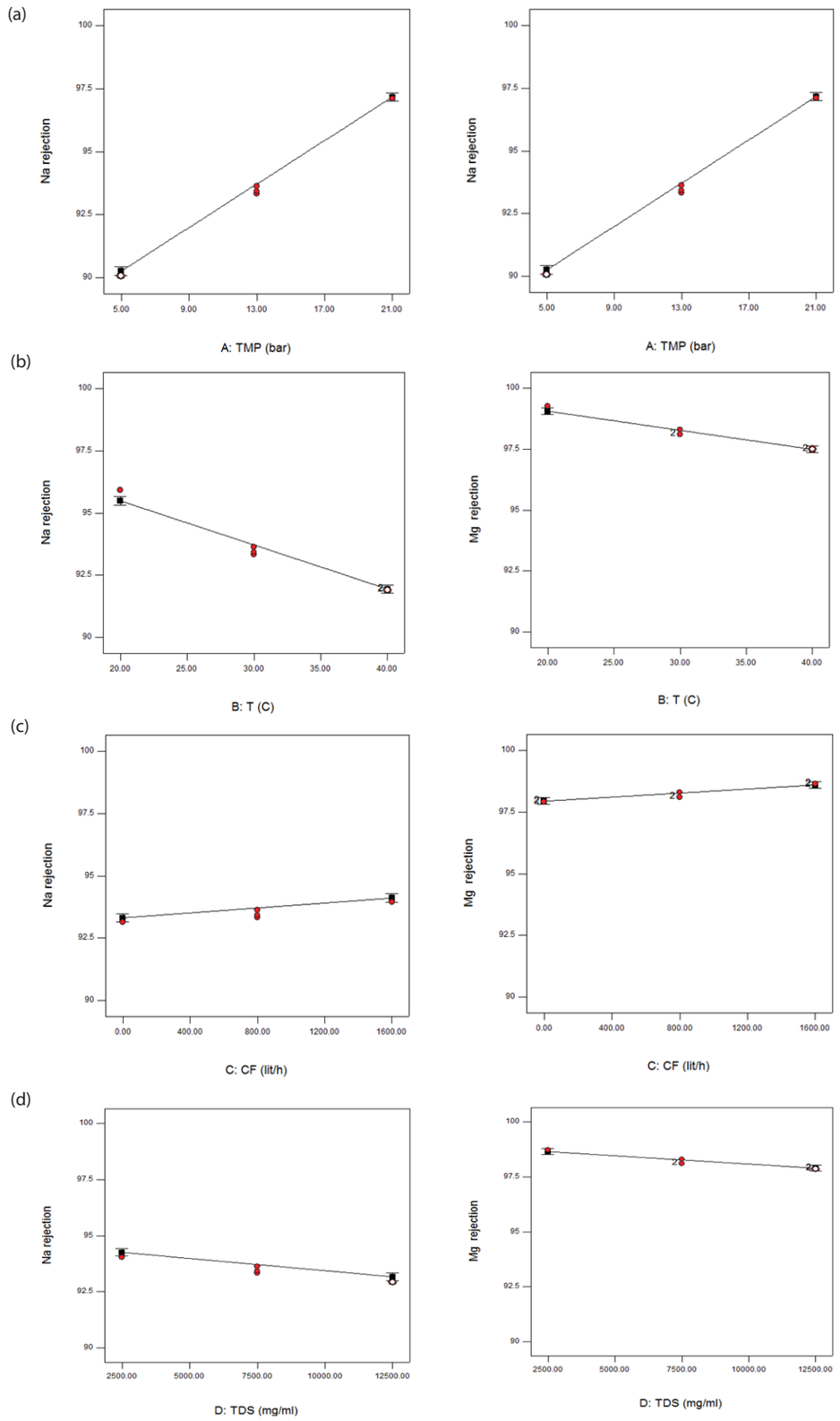

Fig. 4. Effects of TMP, T, CF and TDS on performance of the membrane (solutes rejection) a) T = 35°C, CF = 12000 L·h^{-1} and TDS = 7500 mg·L^{-1}, b) TMP = 17 bar, CF = 12000 L·h^{-1} and TDS = 7500 mg·L^{-1}, c) TMP = 17 bar, T = 35°C and TDS = 7500 mg·L^{-1} and d) TMP = 17 bar, T = 35°C and CF = 12000 L·h^{-1}.

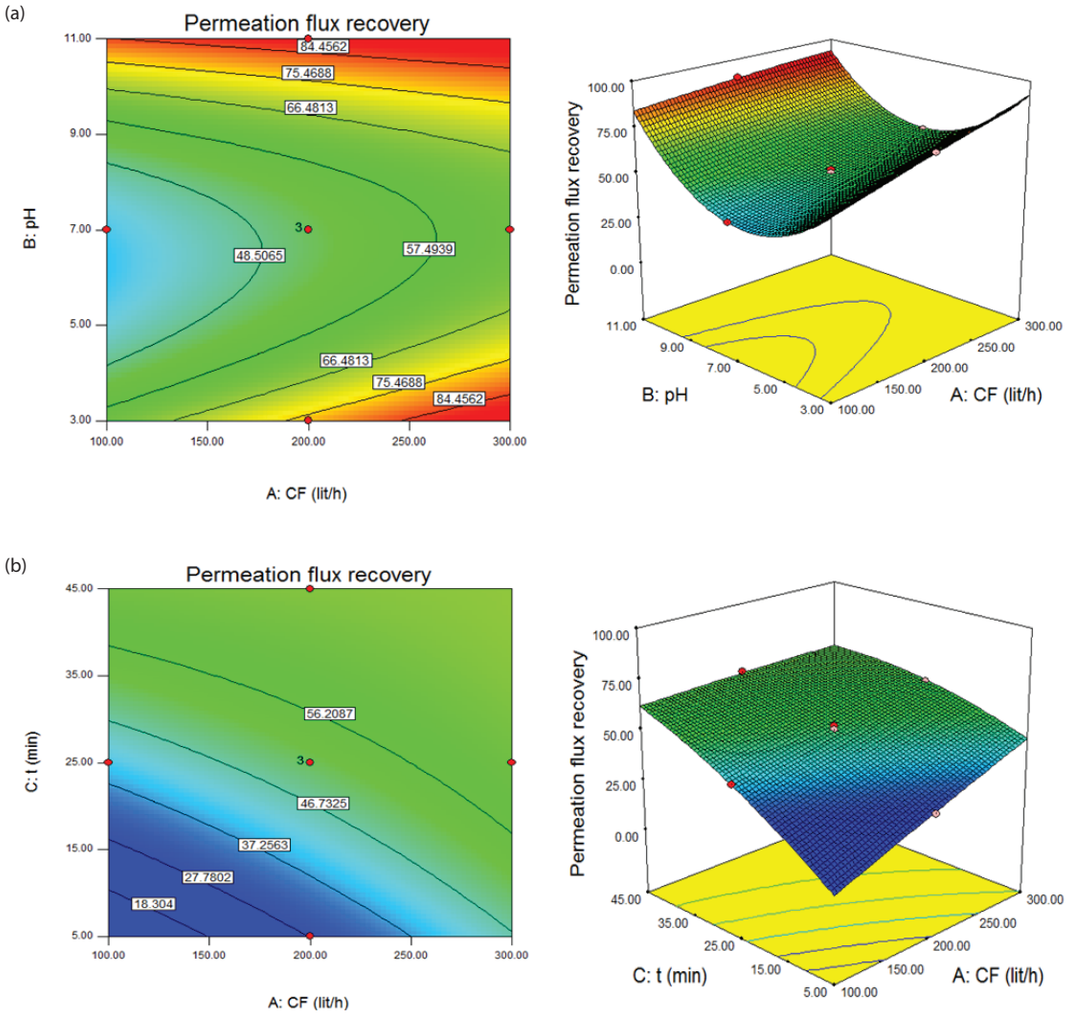

Fig. 5. Effects of CD, pH and t on cleaning of the membrane a) t = 25 min b) and pH = 10.

at the same time increases diffusivity and as a result permeation flux increases [30]. As can be observed, permeation flux increases until 35°C. This can be due to the more significance of viscosity effect than the osmotic pressure effect. However, further increasing temperature results in permeation flux reduction. It can be due to the more significance osmotic pressure effect than the viscosity and diffusivity effects at higher temperature [31]. Based on the results, increasing temperature reduces rejection due to the viscosity effect, as shown in Fig. 5b. In fact at higher temperature, solubility of solutes enhances so more solutes can permeate through the membrane [28,32]. Thus, temperature of 35°C was considered as the optimum value to obtain the higher membrane performance.

4.4.3. Effect of CF

Effect of CF on the permeation flux is shown in Fig. 4c. As it was expected, increasing CF results in the permeation flux increment. It can be attributed to the enhanced flow turbulency that causes the mass transfer coefficient increment and finally decreases the concentration boundary layer thickness formed over the membrane surface [33]. This phenomenon can reduce sediments aggregation in the cake/gel layer so these aggregated materials move back to the feed bulk solution. Thus, concentration polarization effects weakened and the effective pressure difference impact increases [34]. Also, further increasing CF leads to effective pressure difference decrement. Moreover, solutes rejection increases by increasing CF due to the lower concentration of solutes at the membrane surface (Fig. 5c) [18]. Finally, the optimum CF was considered to be12,000 L·h^{-1}.

4.4.4. Effect of TDS

Effects of TDS on performance of the membrane are illustrated in Fig. 4d. The results showed that with increasing the feed TDS, permeation flux is almost constant and further increasing leads to its reduction [35]. It is due to the solute(s) layer formation on the membrane surface quickly and with further increasing it becomes thicker and can partially block the membrane surface. Also, as shown in Fig. 5d,

this reduces the solutes rejections. This decrement is due to the higher concentration gradient of solutes between the feed and permeate sides of the membranes and thus more solutes pass through the membrane. Accordingly, TDS of 10000 mg·L^{-1} was considered as the optimum value [36].

4.5. Cleaning of the membrane

4.5.1. Effect of CF

Effect of CF on cleaning of the membrane was also investigated and is indicated in Fig. 6. As shown, permeation flux recovery increases with CF increment. It can be attributed to the higher shear rates and thus bigger mass transfer coefficients of the cleaning agent through the aggregated materials of cake/gel layer on the membrane surface [37] . As a result, CF of 250 L·h^{-1} was considered as the optimum value of CF.

4.5.2. Effect of pH

The pH effect on the membrane cleaning is also illustrated in Fig. 6. As it can be observed, permeation flux recovery increases with increasing pH [38,39]. Generally, increasing pH results in a more effective interaction between the cleaning agent and the aggregated materials of cake/gel formed foulant layer on the membrane surface. Consequently, the cake/gel layer is cleaned easier. [40]. However, it depends also on the membrane surface physicochemical properties. Higher permeation flux recovery and more chemical stability are the main parameters in determining the optimum pH. Hence, the optimum pH value was considered as 10.

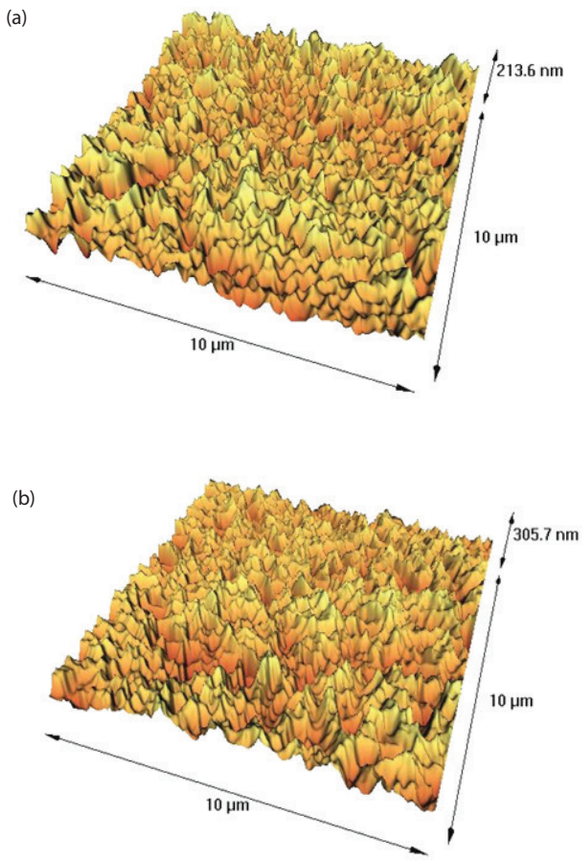

Fig. 6. AFM images of the (a) non-modified and (b) modified membranes.

4.5.3. Effect of cleaning time

Effect of time on cleaning of the fouled membrane is finally presented in Fig. 6. Based on the obtained results, the longer cleaning time lead to the higher permeation flux recovery. It is due to more progress in desirable chemical reactions between the cleaning agent and the aggregated materials of cake/gel layer on the membrane surface as the reaction (cleaning) time increases [41]. So the cleaning time of 45 min was recommended for the cleaning membrane.

4.6. Performance of the membrane at the optimum condition

Optimum values of variables for determining maximum responses for performance and cleaning of the membrane are presented in Table 7. An experiment was performed at the optimum condition in order to investigate the model fitting quality at this condition. For this purpose, the error percentage between the experimental and the related predicted response values was calculated using Eq. (9) as follows:

$$\text{Error (\%)} = \frac{\text{Experimental value} - \text{Predicted value}}{\text{Experimental value}} \times 100 \quad (9)$$

According to the results represented in Table 7, the error percentage calculated from the model is quite small and this means good agreement between the experimental and the predicted results reveals the model suitability.

4.7. Heat treatment

Fouling resistance (i.e. the permeation flux decrease) of non-modified and modified membranes via heat treatment during 20 h are shown in Fig. 8. Permeation flux of the non-modified membrane declines about 20% within this experimental time period. In contrast, permeation flux of the modified membrane has a slight decline of only around 3%. In fact, fouling leads to significant reduction of permeation flux for the non-modified membrane, while the modified membrane permeation flux reveals a negligible reduction. Also, solutes rejections slightly increase. Permeation flux decrement is due to decreasing free-volume hole of the active skin layer and so obtaining denser active skin layer of the modified membrane. Also, slight solutes rejections increment can be explained based on the wetted surface mechanism for mass transfer through the RO membranes, which assumes that the membranes are wetted completely, and thus water molecules as a thin layer stick to the membrane active skin layer by van der Waals forces. This thin water molecules layer penetrates into the internal structure of the active skin layer [3,4]. This phenome-

Table 7
Optimum values of the variables and related predicted and experimental values

	Variables (unit)	Optimum value		Predicted	Experimental	Error (%)
	TMP (bar)	17	Permeation flux ($kg·m^{-2}·h^{-1}$)	57.9	59.1	2
Performance of the membrane	T (°C)	35	Na rejection (%)	94.4	95.0	0.63
	CF ($L·h^{-1}$)	1200	Mg rejection (%)	98.9	99.3	0.40
	TDS ($mg·L^{-1}$)	10000				
Cleaning of the membrane	CF ($L·h^{-1}$)	250	Permeation flux recovery (%)	94.1	94.0	0.10
	pH	10				
	t (min)	45				

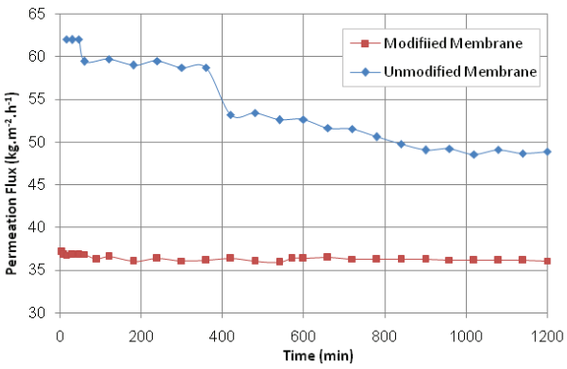

Fig. 7. Fouling resistance results of non-modified and modified membrane during 20 h.

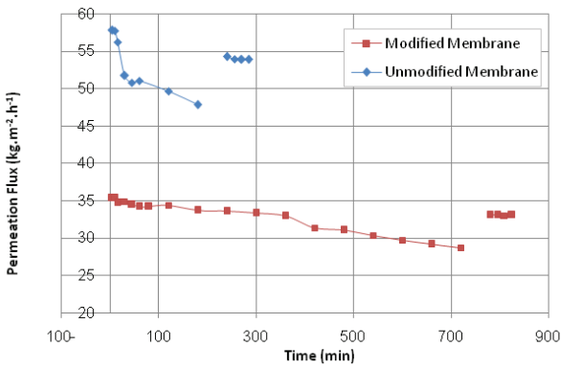

Fig. 8. Cleaning behavior results of non-modified and modified membranes.

non and the denser active skin layer prevent penetration of the foulants through it. Also, increasing surface roughness makes the membrane more hydrophilic and this leads more water molecules stick on the membrane surface and thus less foulants penetrate through the membrane.

Cleaning behavior results of the non-modified and the modified membranes via heat treatment are also indicated in Fig. 8. For this purpose the membranes were fouled using the foulants down to 80% of their initial permeation fluxes. It took about 3 h for the non-modified membrane and approximately 12 h for the modified membrane. Cleaning of the membranes was performed and permeation flux recovery for the non-modified membrane was 94.0% and for the modified membrane was 94.1%. It shows that the interactions the physicochemical characteristics of the both membrane surface and foulants can be reduced and they can be removed better.

5. Conclusion

In this study, RSM by CCD was used to investigate the effects of TMP, T, CF and TDS on performance of a polyamide RO membrane and the effects of CF, pH and *t* on its cleaning behavior. Based on the results, RSM was found as a good approach to optimize the variables. The optimum performance of the membrane with permeation flux of 59.1 $kg·m^{-2}·h^{-1}$ and Na and Mg rejections of 99.3 and 95%, respectively, was identified as TMP of 17 bar, T of 35°C, CF of 1200 $L·h^{-1}$ and TDS of 10000 $mg·L^{-1}$. Also, the optimum permeation flux recovery of 94 % was determined at CF of 250 $L·h^{-1}$, pH of 10 and cleaning time of 45 min. Also, effects of heat treatment as a surface modification method on the fouling resistance and cleaning behavior of the membrane were examined at the optimum condition of performance using experimental design. The non-modified membrane permeation flux decline of about 20% was observed, however the modified membrane permeation flux decline of about 3% was recorded after 20 h of operation. Also, solutes rejections were slightly increased after modification. Also, fouling of the non-modified membrane was observed after 3 h, while that of the modified membrane was observed after 12 h. Permeation flux recovery for the non-modified membrane was 94.0% and for the modified membrane was 94.1%.

Symbols

PF — Permeate flux ($kg·m^{-2}·h^{-1}$)
V — Volume of permeate collected (m^3)
A — Effective membrane area (m^2)
t — Cleaning Time (h)
c_f — Concentration in the feed ($mol·m^{-3}$)
c_p — Concentration in the permeate ($mol·m^{-3}$)
PF_{BF} — Permeation flux before fouling ($kg·m^{-2}·h^{-1}$)

PF_{AC} — Permeation flux after cleaning (kg·m^{-2}·h^{-1})
ΔP — Pressure difference (bar)
μ — Feed viscosity (Pa·s)
ΣR — Summation of resistances in the direction of permeation
$PF_{w\,i}$ — Pure water flux (kg·m^{-2}·h^{-1})
PF_{ww} — The pure water flux through the fouled membrane after filtration (kg·m^{-2}·h^{-1})
Y — Predicted response
x_i and x_j — The independent factors
β_0 — Constant coefficient
$\beta_{i'}$ — Coefficient for linear effect
β_{jj} — Coefficient for quadratic effect
β_{ij} — Coefficient for interaction effect
e_i — Error

References

[1] N.K. Khanzada, S.J. Khan, P.A. Davies, Performance evaluation of reverse osmosis (RO) pre-treatment technologies for in-land brackish water treatment, Desalination, In Press (2016).
[2] S.A. Kalogirou, Seawater desalination using renewable energy sources, Prog. Energ. Combust., 31 (2005) 242–281.
[3] T. Fujioka, N. Oshima, R. Suzuki, M. Higgins, W.E. Price, R.K. Henderson, L.D. Nghiem, Effect of heat treatment on fouling resistance and the rejection of small and neutral solutes by reverse osmosis membranes, Wat. Sci. Technol., 15 (2015) 510–516.
[4] T. Fujioka, L.D. Nghiem, Modification of a polyamide reverse osmosis membrane by heat treatment for enhanced fouling resistance, Wat. Sci. Technol.: Water Supply, 13 (2013) 1553–1559.
[5] N. Ghaffour, T.M. Missimer, G.L. Amy, Technical review and evaluation of the economics of water desalination: current and future challenges for better water supply sustainability, Desalination, 309 (2013) 197–207.
[6] H.R. Mahdavi, M. Arzani, M. Peydayesh, T. Mohammadi, Pertraction of l-lysine by supported liquid membrane using D2EHPA/M2EHPA, Chem. Eng. Process., 106 (2016) 50–58.
[7] A.E. Anqi, N. Alkhamis, A. Oztekin, Steady three dimensional flow and mass transfer analyses for brackish water desalination by reverse osmosis membranes, Int. J. Heat Mass Transfer, 101 (2016) 399–411.
[8] M. Elimelech, The global challenge for adequate and safe water, J. Water Supply Res. T, 55 (2006) 3–10.
[9] J. Morillo, J. Usero, D. Rosado, H. El Bakouri, A. Riaza, F.-J. Bernaola, Comparative study of brine management technologies for desalination plants, Desalination, 336 (2014) 32–49.
[10] T. Qiu, P.A. Davies, Comparison of configurations for high-recovery inland desalination systems, Water, 4 (2012) 690.
[11] C. Garcia, F. Molina, D. Zarzo, 7 year operation of a BWRO plant with raw water from a coastal aquifer for agricultural irrigation, Desal. Water Treat., 31 (2011) 331–338.
[12] C. Fritzmann, J. Löwenberg, T. Wintgens, T. Melin, State-of-the-art of reverse osmosis desalination, Desalination, 216 (2007) 1–76.
[13] A.E. Anqi, N. Alkhamis, A. Oztekin, Numerical simulation of brackish water desalination by a reverse osmosis membrane, Desalination, 369 (2015) 156–164.
[14] K.P. Lee, T.C. Arnot, D. Mattia, A review of reverse osmosis membrane materials for desalination—development to date and future potential, J. Membr. Sci., 370 (2011) 1–22.
[15] L. Malaeb, G.M. Ayoub, Reverse osmosis technology for water treatment: State of the art review, Desalination, 267 (2011) 1–8.
[16] W. Arras, N. Ghaffour, A. Hamou, Performance evaluation of BWRO desalination plant—a case study, Desalination, 235 (2009) 170–178.
[17] G.-d. Kang, Y.-m. Cao, Development of antifouling reverse osmosis membranes for water treatment: A review, Water Res., 46 (2012) 584–600.
[18] A. Rodríguez-Calvo, G.A. Silva-Castro, F. Osorio, J. González-López, C. Calvo, Reverse osmosis seawater desalination: current status of membrane systems, Desal. Water Treat., 56 (2015) 849–861.
[19] R. Gerard, H. Hachisuka, M. Hirose, New membrane developments expanding the horizon for the application of reverse osmosis technology, Desalination, 119 (1998) 47–55.
[20] C. Bartels, M. Wilf, W. Casey, J. Campbell, New generation of low fouling nanofiltration membranes, Desalination, 221 (2008) 158–167.
[21] T. Shintani, H. Matsuyama, N. Kurata, Effect of heat treatment on performance of chlorine-resistant polyamide reverse osmosis membranes, Desalination, 247 (2009) 370–377.
[22] J. Ochando-Pulido, M. Victor-Ortega, A. Martínez-Ferez, On the cleaning procedure of a hydrophilic reverse osmosis membrane fouled by secondary-treated olive mill wastewater, Chem. Eng. J., 260 (2015) 142–151.
[23] A. Bayat, H.R. Mahdavi, M. Kazemimoghaddam, T. Mohammadi, Preparation and characterization of γ-alumina ceramic ultrafiltration membranes for pretreatment of oily wastewater, Desal. Water Treat., 57 (2016) 24322–24332.
[24] M. Arzani, H.R. Mahdavi, O. Bakhtiari, T. Mohammadi, Preparation of mullite ceramic microfilter membranes using response surface methodology based on central composite design, Ceram. Int., 42 (2016) 8155–8164.
[25] J. Kheriji, A. Mnif, I. Bejaoui, B. Hamrouni, Study of the influence of operating parameters on boron removal by a reverse osmosis membrane, Desal. Water Treat., 56 (2015) 2653–2662.
[26] A. Salahi, T. Mohammadi, A. Rahmat Pour, F. Rekabdar, Oily wastewater treatment using ultrafiltration, Desal. Water Treat., 6 (2009) 289–298.
[27] P.V.X. Hung, S.-H. Cho, J.-J. Woo, S.-H. Moon, Behaviors of commercialized seawater reverse osmosis membranes under harsh organic fouling conditions, Desal. Water Treat., 15 (2010) 48–53.
[28] Y.G. Lee, D.Y. Kim, Y.C. Kim, Y.S. Lee, D.H. Jung, M. Park, S.-J. Park, S. Lee, D.R. Yang, J.H. Kim, A rapid performance diagnosis of seawater reverse osmosis membranes: simulation approach, Desal. Water Treat., 15 (2010) 11–19.
[29] M. Sarai Atab, A.J. Smallbone, A.P. Roskilly, An operational and economic study of a reverse osmosis desalination system for potable water and land irrigation, Desalination, 397 (2016) 174–184.
[30] S. Zhao, L. Zou, Effects of working temperature on separation performance, membrane scaling and cleaning in forward osmosis desalination, Desalination, 278 (2011) 157–164.
[31] I. Koyuncu, Effect of operating conditions on the separation of ammonium and nitrate ions with nanofiltration and reverse osmosis membranes, J. Environ. Sci. Health A, 37 (2002) 1347–1359.
[32] B. Girard, L.R. Fukumoto, Membrane Processing of fruit juices and beverages: a review, Crc. Cr. Rev. Food Sci., 40 (2000) 91–157.
[33] S.R. Suwarno, X. Chen, T.H. Chong, D. McDougald, Y. Cohen, S.A. Rice, A.G. Fane, Biofouling in reverse osmosis processes: The roles of flux, crossflow velocity and concentration polarization in biofilm development, J. Membr. Sci., 467 (2014) 116–125.
[34] L. Ding, M.Y. Jaffrin, Benefits of high shear rate dynamic nanofiltration and reverse osmosis: a review, Separ. Sci. Technol., 49 (2014) 1953–1967.
[35] Y. Jang, H. Cho, Y. Shin, Y. Choi, S. Lee, J. Koo, Comparison of fouling propensity and physical cleaning effect in forward osmosis, reverse osmosis, and membrane distillation, Desal. Water Treat., 57 (2016) 24532–24541.
[36] S. Bunani, E. Yörükoğlu, Ü. Yüksel, N. Kabay, M. Yüksel, G. Sert, Application of reverse osmosis for reuse of secondary treated urban wastewater in agricultural irrigation, Desalination, 364 (2015) 68–74.

[37] Z. Wang, J. Tang, C. Zhu, Y. Dong, Q. Wang, Z. Wu, Chemical cleaning protocols for thin film composite (TFC) polyamide forward osmosis membranes used for municipal wastewater treatment, J. Membr. Sci., 475 (2015) 184–192.
[38] C. zum Kolk, W. Hater, N. Kempken, Cleaning of reverse osmosis membranes, Desal. Water Treat., 51 (2013) 343–351.
[39] L.H. Kim, A. Jang, H.-W. Yu, S.-J. Kim, I.S. Kim, Effect of chemical cleaning on membrane biofouling in seawater reverse osmosis processes, Desal. Water Treat., 33 (2011) 289–294.
[40] L. Masse, M. Mondor, J. Puig-Bargués, L. Deschênes, G. Talbot, The efficiency of various chemical solutions to clean reverse osmosis membranes processing swine wastewater, Water Qual. Res. J. Can., 49 (2014) 295–306.
[41] M.S. Camilleri-Rumbau, L. Masse, J. Dubreuil, M. Mondor, K.V. Christensen, B. Norddahl, Fouling of a spiral-wound reverse osmosis membrane processing swine wastewater: effect of cleaning procedure on fouling resistance, Environ. Technol., 37 (2016) 1704–1715.